Il s'agit d'une résonance entre plusieurs états, ce qui contribue à rendre la molécule plus stable. Par ailleurs, cette formule explique parfaitement la présence des pics 279 et 338 trouvés dans le spectre de masse pour cette molécule.

Les auteurs tiennent à remercier M E. F. Bertaut, Directeur du Laboratoire des Rayons X, pour l'intérêt et l'encouragement qu'il porte à leurs travaux.

Références

GERMAIN, G., MAIN, P. & WOOLFSON, M. M. (1970). *Acta Cryst.* B**26**, 274–285.

PERA, M. H. (1974). Thèse Doctorat d'Etat en Pharmacie, N° 4. *Recherche dans la Serie Cyclobutanique. Dérivés de l'Acide Truxillique, Formation de Pyridones-2. Résultats Pharmacologiques.* Université Scientifique et Médicale de Grenoble.

PERA, M. H., TRANQUI, D., FILLION, H. & LUU DUC, C. (1975). *Bull. Soc. Chim. Fr.* pp. 321–323.

Acta Cryst. (1976). B**32**, 1727

The Structure of a Trinucleoside Diphosphate: Adenylyl-(3′,5′)-adenylyl-(3′,5′)-adenosine Hexahydrate

BY D. SUCK,* P. C. MANOR† AND W. SAENGER‡

Chemische Abteilung, Max-Planck-Institut für experimentelle Medizin, 3400 Göttingen, Germany (BRD)

(*Received* 27 *October* 1975; *accepted* 28 *November* 1975)

The title compound (ApApA) constitutes a fragment of polyadenylic acid (poly A). It was crystallized from acidic solution in space group $P4_12_12$ with $a=14{\cdot}155$, $c=44{\cdot}00$ Å, $Z=8$ and in space group $P4_1$, $a=14{\cdot}080$, $c=44{\cdot}04$ Å, $Z=8$. 3260 reflexions to 0·95 Å resolution were collected for $P4_12_12$ with a diffractometer; the structure was solved by direct methods and refined by least-squares cycles to $R=6{\cdot}8$ %. In the crystal structure, the middle and 3′-terminal adenine heterocycles are protonated at N(1) giving rise to a zwitterion of the form ApA^+pA^+ and two of these molecules are complexed *via* $A^+.A^+$ base pairs similar to those found in the poly A^+ duplex. In the latter structure the polynucleotide chains are arranged parallel but in the ApA^+pA^+ dimer, the molecules are antiparallel (diad related), causing a non-helical structure. The adenosines are in the normal C(3′)-*endo*, *gauche*, *gauche* and *anti* conformation; the orientation about the P–O ester bonds is helical, (−)*gauche*, (−)*gauche* for ApA^+ but non-helical, looped (+)*gauche*, (+)*gauche* for A^+pA^+. The latter structure is stabilized by a hydrogen bond between the 3′-terminal O(3′)–H hydroxyl group and the penultimate phosphate group. All the bases of the dimer are stacked to form a hydrophobic core which is surrounded by the hydrophilic ribose and phosphate groups. The dimer is embedded in 12 water molecules, several of them being statistically disordered. From the helical ApA^+ fragment a structural model for single helical, unprotonated poly A could be derived: nine nucleotides constitute a pitch of 25·4 Å; the adenine heterocycles are tilted by 24° *versus* the helix axis.

Introduction

Ribonucleic acids (RNA's) play a central role in the transfer of genetic information. They occur either as single-stranded molecules with unknown secondary structure or they form double helical complexes (Watson & Crick, 1953) with complementary A:U and G:C base pairing and antiparallel oriented polynucleotide chains related to each other by a diad perpendicular to the helix axis. The synthetic homopolymer polyadenylic acid (poly A) exhibits short single helical regions at neutral *p*H (Brahms, Michelson & van Holde, 1966) while under acidic conditions it becomes protonated at N(1) of the adenine bases and assumes a double helical structure. Unlike Watson–Crick duplexes, however, the poly A^+ chains in the poly A^+.poly A^+ duplex are arranged parallel to each other and related by a diad coinciding with the helix axis (Fig. 1) (Rich, Davies, Crick & Watson, 1961).

Crystallization of the poly A fragment adenylyl-(3′,5′)-adenylyl-(3′,5′-)-adenosine (ApApA) (Fig. 2) in acidic conditions was undertaken in order to obtain a short piece of a double helical poly A^+.poly A^+ complex. In this contribution, details of the structure analyses are described; a preliminary report on the biochemical significance of this study has appeared (Suck, Manor, Germain, Schwalbe, Weimann & Saenger, 1973). Information from single-crystal studies is only available on some diribonucleoside phosphates (Shefter, Barlow, Sparks & Trueblood, 1969; Rubin, Brennan & Sundaralingam, 1972; Sussman, Seeman,

* Present address: Dept. of Biological Sciences, Purdue University, West Lafayette, Indiana, U.S.A.

† Present address: Dept. of Biochemical Sciences, Princeton University, Princeton, New Jersey, U.S.A.

‡ To whom correspondence should be addressed.

Kim & Berman, 1972; Day, Seeman, Rosenberg & Rich, 1973; Rosenberg, Seeman, Kim, Suddath, Nicholas & Rich, 1973; Stellman, Hingerty, Broyde, Subramanian, Sato & Langridge, 1973; Tsai, Jain & Sobell, 1975; Seeman, Day & Rich, 1975) and on a dideoxynucleotide (Camerman, Fawcett & Camerman, 1973). The X-ray structure of ApApA (Fig. 1) therefore gives information exceeding the dinucleotide level.

Experimental

The ammonium salt of ApApA was provided by Dr G. Weimann (Boehringer, Tutzing). For crystallization aqueous solutions of ApApA were adjusted to *p*H 2·8 to 3·2 by addition of various acids. The crystals obtained were invariably truncated tetragonal pyramids or bipyramids, regardless of the acid or the cations used. Despite their similar habit, the crystals belong to two different tetragonal space groups, $P4_12_12$ and $P4_1$, with slightly different cell constants (Table 1) and one and two ApApA molecules per asymmetric unit, respectively. The diffraction patterns for both crystal types are comparable, but deviations from the *p4m* symmetry in the *hk*0 photographs of the $P4_1$ crystals are obvious. For the $P4_12_12$ crystals the observed and calculated densities are in good agreement if one assumes the asymmetric unit to contain one ApApA molecule plus six water molecules.

Table 1. *Crystal data*

$C_{30}H_{37}N_{15}O_{16}P_2.6H_2O$, M.W. 1033·78

Space group $P4_12_12$, $Z=8$
$a=14{\cdot}155$ (5) Å
$c=44{\cdot}00$ (2)
Cu $K\alpha$ radiation $\lambda=1{\cdot}54182$ Å
$\varrho_o=1{\cdot}553$ g cm^{-3} (flotation method)
$\varrho_c=1{\cdot}559$
Crystal size $0{\cdot}1\times0{\cdot}1\times0{\cdot}3$ mm
$\mu=17{\cdot}94$ cm^{-1}

Space group $P4_1$
$Z=8$ (two molecules per asymmetric unit)
$a=14{\cdot}080$ (4) Å
$c=44{\cdot}04$ (2)

Data have been collected for both crystal types, but only the $P4_12_12$ crystals will be described here in detail. Crystals, $0{\cdot}1\times0{\cdot}1\times0{\cdot}3$mm, were sealed with some mother liquor in quartz capillaries. 3260 intensities up to a resolution of 0·95 Å were measured with Cu $K\alpha$ radiation on an automatic Stoe four-circle diffractometer with the $\theta,2\theta$-scan method and stationary background counts on each side of the scans. Two check reflexions were monitored during data collection at intervals of about one hour. The intensities were corrected for geometrical factors but not for absorption.

Structure determination and refinement

Oscillation photographs taken with the crystallographic *c* axis coinciding with the spindle axis showed prominent reflexions close to **c** at a spacing of 3·7 Å and resembled X-ray fibre diagrams of nucleic acids. Since the distribution of peak densities in the Patter-

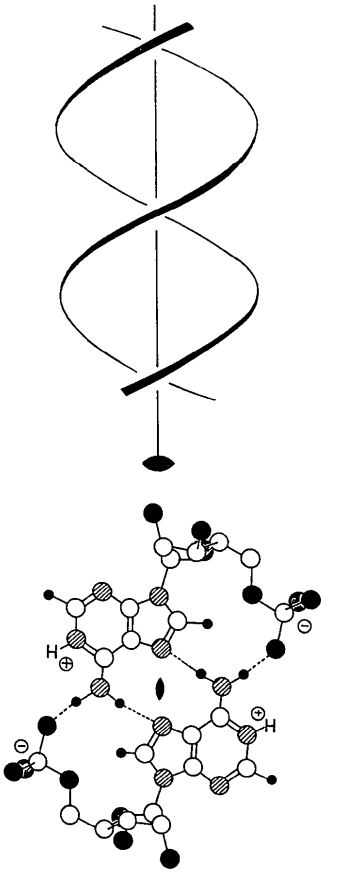

Fig. 1. Schematic representation of the poly A$^+$.poly A$^+$ base pair and double helix.

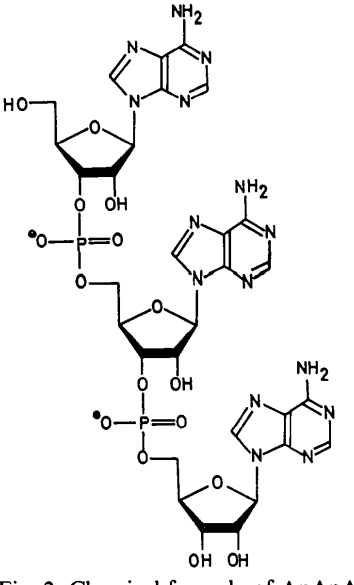

Fig. 2. Chemical formula of ApApA.

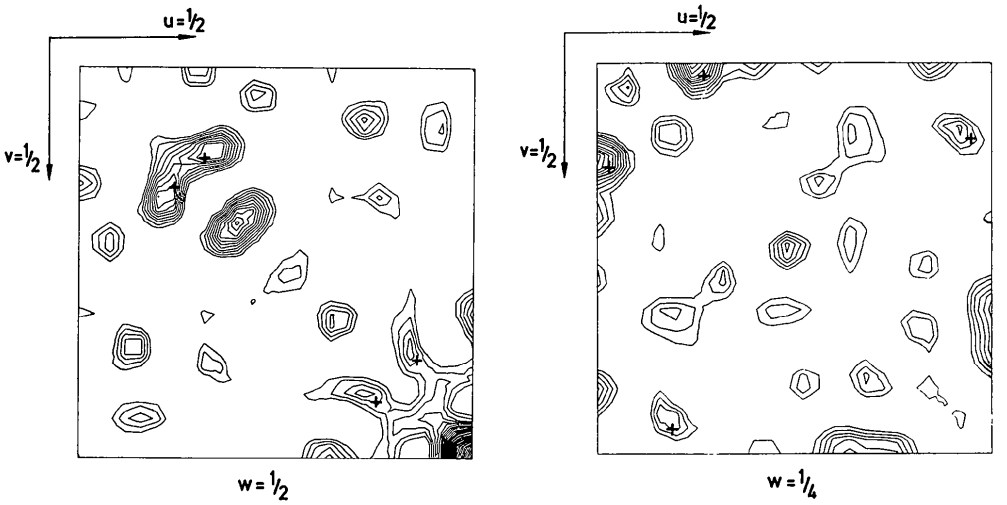

Fig. 3. Harker sections at $w=\frac{1}{2}$ (left) and $w=\frac{1}{4}$ (right). Peaks corresponding to the final P positions are marked by crosses. Contour lines are drawn at equidistant intervals.

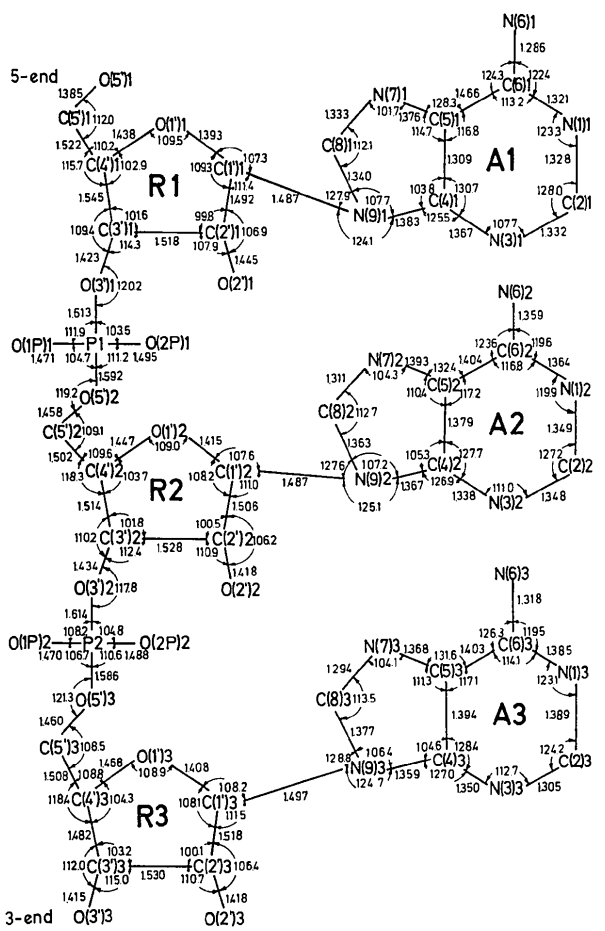

Fig. 4. Bond angles and distances in ApA^+pA^+. Averaged estimated standard deviations are 0·005 Å and 0·3° for bonds and angles involving the P atoms and 0·01 Å and 0·6° for the other bonds and angles. The following angles are not shown: O(3′)–P11–O(5′)2 105·3, O(1P)1–P1–P(2P)2 119·5, O(3′)2–P2–O(5′)2 103·9, O(1P)2–P2–O(2P)2 121·3°.

son map also indicated layers of atoms at 3·7 Å distance along **c**, we expected an arrangement of the ApApA molecules similar to that in double helical poly A^+.poly A^+ complexes with base pairs perpendicular to **c** and at 3·7 Å separation from each other. This structure however requires a diad perpendicular to the adenine base pairs, *i.e.* parallel to **c**, a situation inconsistent with the space group symmetry which exhibits diads perpendicular to **c**, and a strong indication that ApApA did not crystallize as expected. Nevertheless, we assumed that there should be some interbase hydrogen bonding like that proposed for poly A^+ (Fig. 1) (Rich *et al.*, 1961). Attempts were made, therefore, to solve the structure with vector search methods (Nordman, 1966) based on this adenine base pair. Unfortunately, the results were ambiguous and Fourier calculations for various possible locations of the search group did not reveal further parts of the structure. Similarly, our attempts to locate the phosphate groups from an origin-removed, normal sharpened Patterson map failed, even though the actual P positions correspond to prominent Harker peaks (Fig. 3).

After these discouraging results with Patterson methods, direct methods were applied with *MULTAN* (Main, Germain & Woolfson, 1971; Germain & Woolfson, 1968). The starting set chosen by the program consisted of five reflexions including two origin-fixing reflexions. 16 phase sets were obtained for the 437 strongest normalized structure factors, $E>1{\cdot}44$ (Karle & Hauptman, 1956), two of which were almost identical and had clearly better figures of merit than the others. The E map calculated with one of these two phase sets contained 25 peaks in chemically meaningful positions, besides a number of spurious peaks. Among these 25 peaks we could identify the middle adenine ring, the phosphate groups and a few atoms of the attached ribose units. The remaining atoms of the molecule with the hydration water O atoms could be lo-

Table 2. *Fractional atomic coordinates and thermal parameters of the form* $T = exp\,[-(\beta_{11}h^2+\beta_{22}k^2+\beta_{33}l^2+2\beta_{12}hk+2\beta_{13}hl+2\beta_{23}kl)]$

Isotropic temperature factors are given for the hydrogen atoms. The β's are multiplied by 10^4, except for β_{33} which is multiplied by 10^5. Estimated standard deviations for the last decimal place are given in parentheses.

	x	y	z	β_{11}	β_{22}	β_{33}	β_{12}	β_{13}	β_{23}
N(1)1	0·8759 (5)	0·6960 (5)	0·1163 (2)	85 (5)	62 (5)	78 (5)	−1 (5)	1 (1)	2 (1)
C(2)1	0·8156 (10)	0·7481 (8)	0·1322 (2)	128 (10)	66 (6)	93 (7)	−35 (6)	−4 (2)	6 (2)
N(3)1	0·7263 (6)	0·7280 (5)	0·1393 (2)	87 (5)	74 (5)	89 (5)	−22 (5)	−2 (2)	3 (1)
C(4)1	0·7072 (6)	0·6391 (6)	0·1288 (2)	85 (6)	58 (5)	56 (5)	6 (5)	−5 (2)	2 (1)
C(5)1	0·7594 (6)	0·5802 (5)	0·1132 (2)	75 (5)	53 (5)	58 (5)	−1 (5)	−5 (2)	4 (1)
O(6)1	0·8567 (8)	0·6096 (6)	0·1067 (2)	89 (6)	69 (6)	51 (5)	1 (5)	0 (2)	5 (1)
N(6)1	0·9170 (5)	0·5592 (6)	0·0920 (2)	75 (5)	127 (8)	84 (5)	4 (5)	4 (2)	9 (2)
N(7)1	0·7165 (5)	0·4955 (5)	0·1064 (2)	81 (5)	68 (5)	76 (5)	16 (5)	−2 (1)	1 (1)
C(8)1	0·6324 (6)	0·5059 (5)	0·1197 (2)	71 (6)	51 (5)	69 (5)	12 (5)	−3 (2)	0 (1)
N(9)1	0·6233 (5)	0·5908 (5)	0·1329 (2)	56 (5)	69 (5)	76 (5)	−9 (4)	−4 (1)	7 (1)
C(1′)1	0·5438 (6)	0·6255 (6)	0·1520 (2)	80 (5)	68 (5)	69 (5)	−1 (5)	−4 (2)	1 (2)
C(2′)1	0·4896 (4)	0·7015 (4)	0·1362 (1)	63 (4)	59 (4)	69 (2)	4 (2)	−4 (1)	0 (1)
O(2′)1	0·4396 (5)	0·7536 (5)	0·1595 (2)	128 (5)	92 (5)	138 (5)	26 (5)	−6 (1)	−16 (1)
O(1′)1	0·4843 (5)	0·5489 (5)	0·1574 (2)	67 (6)	73 (5)	58 (7)	3 (5)	−1 (2)	7 (2)
C(3′)1	0·4180 (5)	0·6418 (5)	0·1191 (2)	43 (4)	53 (5)	51 (3)	1 (4)	−2 (1)	4 (1)
O(3′)1	0·3337 (2)	0·6906 (4)	0·1111 (1)	45 (2)	62 (2)	47 (2)	12 (2)	2 (1)	4 (1)
C(4′)1	0·3947 (5)	0·5647 (5)	0·1429 (2)	47 (5)	62 (5)	63 (5)	3 (4)	1 (1)	5 (1)
C(5′)1	0·3563 (6)	0·4724 (6)	0·1302 (2)	60 (6)	74 (5)	89 (7)	−13 (5)	2 (2)	9 (2)
O(5′)1	0·4141 (5)	0·4356 (5)	0·1077 (2)	110 (5)	65 (4)	89 (5)	−20 (4)	0 (1)	0 (1)
P1	0·3124 (1)	0·7162 (1)	0·0760 (0)	28 (1)	32 (1)	47 (0)	−1 (1)	0 (0)	1 (0)
O(1P)2	0·3448 (2)	0·6412 (2)	0·0553 (1)	43 (2)	40 (2)	61 (2)	−1 (2)	−1 (1)	0 (1)
O(2P)1	0·2104 (2)	0·7438 (2)	0·0762 (1)	30 (2)	47 (2)	70 (2)	−2 (2)	0 (1)	2 (1)
N(1)2	0·9131 (4)	0·7705 (5)	0·0388 (2)	35 (4)	45 (4)	81 (5)	2 (2)	2 (1)	−1 (1)
C(2)2	0·9003 (5)	0·8533 (5)	0·0534 (2)	42 (5)	50 (5)	69 (5)	−13 (4)	2 (1)	−3 (1)
N(3)2	0·8183 (4)	0·8889 (4)	0·0640 (1)	27 (2)	44 (4)	67 (3)	0 (2)	0 (1)	−1 (1)
C(4)2	0·7466 (5)	0·8293 (5)	0·0589 (2)	27 (4)	31 (4)	52 (3)	2 (2)	1 (1)	1 (1)
C(5)2	0·7498 (4)	0·7427 (5)	0·0446 (2)	23 (4)	27 (4)	57 (5)	4 (2)	0 (1)	1 (1)
C(6′)2	0·8383 (5)	0·7114 (5)	0·0342 (2)	31 (4)	32 (4)	63 (5)	−3 (2)	−1 (1)	0 (1)
N(6)2	0·8520 (4)	0·6270 (4)	0·0202 (1)	37 (2)	41 (4)	66 (3)	9 (2)	1 (1)	−2 (1)
N(7)2	0·6602 (4)	0·7019 (4)	0·0439 (1)	33 (2)	32 (2)	63 (3)	2 (2)	1 (1)	−2 (1)
C(8)2	0·6054 (5)	0·7648 (5)	0·0569 (2)	28 (4)	35 (4)	63 (5)	2 (2)	2 (1)	0 (1)
N(9)2	0·6538 (4)	0·8427 (4)	0·0664 (1)	30 (2)	28 (2)	45 (2)	0 (2)	2 (1)	−3 (1)
C(1′)2	0·6146 (5)	0·9296 (4)	0·0806 (2)	33 (4)	24 (2)	58 (3)	−4 (2)	0 (1)	0 (1)
O(1′)2	0·5308 (2)	0·9040 (2)	0·0960 (1)	34 (2)	32 (2)	46 (2)	2 (2)	1 (1)	1 (1)
C(2′)2	0·5899 (5)	1·0020 (5)	0·0568 (2)	32 (4)	26 (4)	57 (3)	−2 (2)	0 (1)	−1 (1)
O(2′)2	0·5965 (2)	1·0913 (2)	0·0713 (1)	50 (2)	24 (2)	69 (2)	−10 (2)	−1 (1)	−1 (1)
C(3′)2	0·4868 (5)	0·9762 (5)	0·0506 (1)	35 (4)	27 (4)	45 (3)	3 (2)	1 (1)	1 (1)
O(3′)2	0·4340 (2)	1·0538 (2)	0·0383 (1)	42 (2)	30 (2)	52 (2)	6 (2)	0 (1)	0 (1)
C(4′)2	0·4516 (5)	0·9523 (5)	0·0822 (2)	34 (4)	24 (4)	57 (3)	5 (2)	0 (1)	−1 (1)
C(5′)2	0·3643 (5)	0·8926 (5)	0·0851 (2)	29 (4)	37 (4)	62 (5)	0 (2)	3 (1)	−1 (1)
O(5′)2	0·3783 (2)	0·8043 (2)	0·0686 (1)	36 (2)	33 (2)	44 (2)	−9 (2)	1 (1)	0 (1)
P2	0·4216 (1)	1·0590 (1)	0·0019 (0)	47 (1)	25 (1)	50 (0)	4 (1)	0 (0)	0 (0)
O(1)P2	0·5092 (4)	1·0245 (4)	−0·0122 (1)	64 (4)	55 (2)	56 (2)	8 (2)	5 (1)	3 (1)
O(2P)2	0·3858 (1)	1·1561 (2)	−0·0041 (1)	65 (4)	31 (2)	72 (3)	2 (2)	−2 (1)	3 (1)
N(1)3	0·4002 (4)	0·4680 (4)	−0·0407 (2)	30 (2)	33 (2)	75 (3)	−1 (2)	1 (1)	−1 (1)
C(2)3	0·3036 (5)	0·4829 (5)	−0·0432 (2)	27 (4)	38 (5)	89 (5)	−5 (2)	1 (1)	2 (1)
N(3)3	0·2631 (4)	0·5654 (4)	−0·0406 (2)	27 (2)	31 (4)	91 (5)	−2 (2)	1 (1)	0 (1)
C(4)3	0·3253 (5)	0·6353 (5)	−0·0346 (2)	40 (4)	30 (4)	51 (3)	4 (2)	1 (1)	0 (1)
C(5)3	0·4232 (5)	0·6294 (5)	−0·0318 (2)	26 (4)	30 (4)	53 (3)	1 (2)	0 (1)	−1 (1)
C(6)3	0·4647 (5)	0·5405 (5)	−0·0366 (2)	35 (5)	39 (4)	50 (3)	−7 (2)	0 (1)	1 (1)
N(6)3	0·5558 (4)	0·5217 (4)	−0·0370 (1)	27 (2)	39 (2)	64 (3)	9 (2)	1 (1)	0 (1)
N(7)3	0·4619 (4)	0·7156 (4)	−0·0252 (1)	24 (2)	39 (2)	68 (3)	0 (2)	1 (1)	−1 (1)
C(8)3	0·3900 (5)	0·7717 (5)	−0·0235 (2)	37 (4)	34 (4)	76 (5)	−2 (4)	−1 (1)	−3 (1)
N(9)3	0·3052 (4)	0·7280 (4)	−0·0298 (1)	22 (2)	37 (2)	56 (2)	0 (2)	1 (1)	−1 (1)
C(1′)3	0·2079 (5)	0·7694 (5)	−0·0298 (2)	25 (4)	36 (4)	64 (5)	5 (2)	−2 (1)	−1 (1)
O(1′)3	0·2155 (2)	0·8668 (2)	−0·0360 (1)	49 (2)	36 (2)	56 (2)	11 (2)	−3 (1)	0 (1)
C(2′)3	0·1602 (5)	0·7579 (5)	0·0008 (2)	28 (4)	58 (5)	52 (3)	−2 (2)	1 (1)	−2 (1)
O(2′)3	0·0616 (4)	0·7570 (5)	−0·0048 (1)	39 (2)	95 (5)	86 (3)	−11 (2)	2 (1)	−12 (1)
C(3′)3	0·1897 (5)	0·8506 (5)	0·0160 (2)	41 (4)	48 (4)	43 (3)	5 (2)	−1 (1)	−4 (1)
O(3′)3	0·1337 (2)	0·8781 (4)	0·0412 (1)	44 (2)	67 (2)	60 (2)	9 (2)	1 (1)	−6 (1)
C(4′)3	0·1846 (5)	0·9201 (5)	−0·0092 (2)	49 (4)	35 (4)	54 (5)	18 (2)	−2 (1)	−2 (1)
C(5′)3	0·2427 (5)	1·0091 (5)	−0·0068 (2)	54 (5)	41 (4)	66 (5)	7 (4)	−3 (1)	−2 (1)
O(5′)3	0·3424 (4)	0·9829 (2)	−0·0052 (1)	58 (2)	29 (2)	79 (3)	5 (2)	−7 (1)	0 (1)

Table 2 (*cont.*)

O*W*(1)	0·0924 (5)	0·5824 (5)	0·0650 (2)	84 (5)	111 (5)	100 (5)	−32 (4)	1 (1)	−3 (1)
O*W*(2)	0·2911 (4)	0·4648 (4)	0·0389 (2)	49 (4)	62 (4)	190 (7)	17 (2)	−12 (1)	−15 (1)
O*W*(4)	0·8981 (8)	0·3712 (6)	0·0794 (2)	179 (8)	125 (6)	123 (5)	2 (6)	−13 (2)	−4 (2)
O*W*(6)	0·0677 (6)	0·7398 (8)	0·1201 (2)	119 (6)	194 (10)	137 (7)	−65 (6)	15 (2)	−10 (2)
O*W*(3)	0·2519 (6)	0·2340 (8)	0·0344 (2)	62 (5)	95 (8)	198 (11)	11 (5)	−3 (2)	−10 (2)
O*W*(5)1	0·2993 (13)	0·2680 (16)	0·0893 (5)	86 (11)	121 (17)	127 (14)	−39 (11)	19 (4)	−2 (4)
O*W*(5)2	0·3238 (16)	0·1719 (19)	0·0849 (5)	69 (13)	111 (19)	208 (23)	−49 (13)	4 (3)	−2 (5)
O*W*(7)	0·1527 (8)	0·4142 (8)	0·0897 (2)	100 (8)	119 (8)	86 (7)	−45 (6)	0 (2)	7 (2)

Table 2 (*cont.*)

	x	*y*	*z*	*B*
H(2)1	0·843	0·812	0·140	8·96
H(8)1	0·587	0·450	0·120	4·49
H(1′)1	0·572	0·650	0·171	5·31
H(2′)1	0·531	0·745	0·122	5·08
H(3′)1	0·448	0·612	0·100	3·39
H(4′)1	0·347	0·592	0·158	5·23
H(5′)1	0·348	0·425	0·147	5·77
H(5′)1	0·289	0·483	0·122	5·77
H(2)2	0·961	0·893	0·056	3·79
H(8)2	0·535	0·756	0·060	2·52
H(1′)2	0·662	0·958	0·096	3·13
H(2′)2	0·632	0·996	0·038	2·37
H(3′)2	0·483	0·918	0·037	2·21
H(4′)2	0·441	1·012	0·094	3·09
H(5′)2	0·309	0·929	0·077	2·68
H(5′)2	0·351	0·879	0·107	2·69
H(1)3	0·426	0·401	−0·042	2·82
H(2)3	0·261	0·426	−0·048	3·06
H(8)3	0·396	0·842	−0·018	3·37
H(1′)3	0·168	0·740	−0·047	2·40
H(2′)3	0·183	0·700	0·012	3·53
H(3′)3	0·258	0·847	0·023	3·76
H(4′)3	0·116	0·937	−0·012	3·50
H(5′)3	0·230	1·052	−0·025	3·60

cated by phase refinement with the tangent formula (Karle & Hauptman, 1956) and a series of Fourier and difference syntheses. Full-matrix least-squares refinement (Busing, Martin & Levy, 1962) converged after three cycles of isotropic and eight cycles of anisotropic refinement at $R=\sum||F_o|-|F_c||/\sum|F_o|=6{\cdot}4\%$ for the 3210 significant reflexions and 6·8% for all 3260 data. The weighting scheme applied was based on counter statistics with a 2% allowance for machine instability (Stout & Jensen, 1968) and reflexions with $F_o \leq 3\sigma(F_o)$ were considered unobserved and not included in the refinement. Only 22 out of 37 H atoms could be located from difference maps; they were included in the refinement with the isotropic temperature factors of those atoms to which they are bound.

With the atomic positions derived from the $P4_12_12$ structure we could solve the $P4_1$ structure and refine

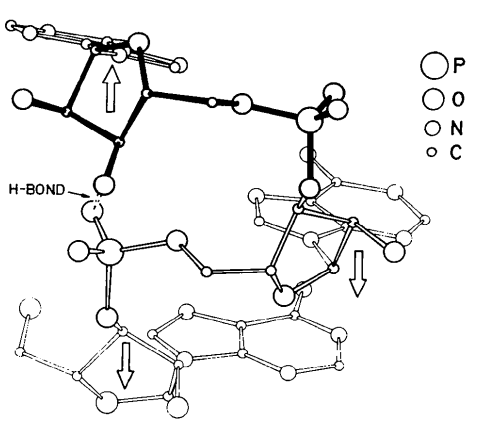

Fig. 5. View of the ApA^+pA^+ molecule in a direction perpendicular to the fourfold screw axis, demonstrating the helical arrangement of the 5′-terminal (top) and middle (centre) adenosines and the folding back of the 3′-terminal (bottom) adenosine. The arrows indicate the orientations of the riboses relative to each other. The O(3′)–H···O⁻–P hydrogen bond is marked by a dotted line.

Table 3. *Deviations from least-squares planes through adenine and ribose rings*

The plane-defining atoms are marked by an asterisk.

(*a*) Adenine bases

Plane equations

A1 $0{\cdot}3337X-0{\cdot}3913Y+0{\cdot}8576Z-4{\cdot}674=0$
A2 $0{\cdot}1682X+0{\cdot}4402Y-0{\cdot}8820Z-1{\cdot}1090=0$
A3 $0{\cdot}0922X+0{\cdot}1766Y-0{\cdot}9800Z-3{\cdot}4865=0$

Deviations from plane (Å)

	A1	A2	A3
N(1)*	−0·004	0·012	−0·042
C(2)*	0·023	−0·008	−0·023
N(3)*	0·021	−0·002	−0·020
C(4)*	−0·013	−0·005	0·016
C(5)*	−0·030	0·004	0·008
C(6)*	0·024	−0·001	0·050
N(6)*	0·033	−0·013	0·138
N(7)*	−0·018	−0·012	−0·009
C(8)*	0·027	0·006	−0·037
N(9)*	0·013	0·007	0·016
C(1′)	0·164	0·091	−0·006

Angles between planes

A1/A2 10·0°
A1/A3 28·5
A2/A3 22·1

(*b*) Ribose rings

Plane equations

R1 $-0{\cdot}3253X+0{\cdot}3788Y+0{\cdot}8664Z-6{\cdot}6786=0$
R2 $0{\cdot}1202X+0{\cdot}7420Y+0{\cdot}6595Z-13{\cdot}1634=0$
R3 $0{\cdot}9111X-0{\cdot}0407Y+0{\cdot}4101Z-1{\cdot}6640=0$

Deviations from plane (Å)

	R1	R2	R3
C(1′)*	−0·036	−0·018	0·034
C(2′)*	0·021	0·011	−0·020
O(1′)*	0·037	0·018	−0·035
C(4′)*	−0·022	−0·011	0·021
C(3′)	−0·621	−0·616	0·581
O(2′)	1·416	1·379	−1·393
O(3′)	−0·277	−0·247	0·296
C(5′)	−0·824	−0·702	0·761

Table 4. *Dihedral angles* (°)

		A1	A2	A3		
(*a*) Ribose, endocyclic						
	C(1′)–C(2′)–C(3′)–C(4′)	39·2	38·8	38·1		
	C(2′)–C(3′)–C(4′)–O(1′)	−36·6	−38·0	−35·7		
	C(3′)–C(4′)–O(1′)–C(1′)	18·9	22·0	18·7		
	C(4′)–O(1′)–C(1′)–C(2′)	6·9	3·4	6·3		
	O(1′)–C(1)′–C(2′)–C(3′)	−29·7	−26·8	−27·5		
(*b*) Glycosidic bond						
	C(8) –N(9)–C(1′)–O(1′)	8·1	28·2	26·6		
	C(2′)–C(1′)–N(9)–C(4)	76·5	85·7	83·8		
(*c*) Phosphate sugar backbone						
		A1/A2	A2/A3	A3	UpA	A-RNA*
	P——O(5′)–C(5′)–C(4′)	161·1	−171·7	–	−157	180
	O(5′)–C(5′)–C(4′)–O(1′)	−63·4	−62·7	−57·6		
	O(5′)–C(5′)–C(4′)–C(3′)	52·8	55·9	61·1		
	C(5′)–C(4′)–C(3′)–O(3′)	82·0	81·0	79·0		
	C(4′)–C(3′)–O(3′)–P	−137·1	−150·7	–	−154	−151
ω'	C(3′)–O(3′)–P——O(5′)	−176·7	77·2		81	−74
ω	O(3′)–P——O(5′)–C(5′)	−62·5	92·8		82	−62

* 11-fold double helical A-RNA (Arnott & Hukins, 1972)

it by isotropic least squares to $R=17\%$. Both structures are very similar and there are only slight differences in the positions of the 5′-terminal adenosine and the hydration water molecules. In this contribution only the $P4_12_12$ structure will be discussed in detail.

Results and discussion

In Tables 2 to 5 the final atomic parameters, deviations from least-squares planes, dihedral angles and short intermolecular distances are listed.* Figs. 4 to 9 present angles and distances in ApApA, a view of the single ApApA molecule in a direction perpendicular to **c**, the ApApA molecule projected along **c** with the 3′-terminal adenosine rotated into a helical position,

* A list of structure factors has been deposited with the British Library Lending Division as Supplementary Publication No. SUP 31540 (20 pp., 1 microfiche). Copies may be obtained through The Executive Secretary, International Union of Crystallography, 13 White Friars, Chester CH1 1NZ, England.

Table 5. *Hydrogen bonds and short intermolecular distances* (Å)

N(1)1 · · · · O(2′)2^{i}	3·140	N(7)2 · · · · · N(6)3^{v}	2·864
N(1)1 · · · · O*W*(6)^{ii}	2·789	O(2′)2 · · · · · N(3)3^{vii}	2·816
N(3)1 · · · · O*W*(4)^{iii}	3·016	O(3′)2 · · · · · O*W*(5)2^{viii}	3·069
N(6)1 · · · · O*W*(1)^{ii}	2·771	O(2P)2 · · · · O*W*(2)^{v}	2·692
N(2′)1 · · · · O*W*(4)^{iii}	2·878	O(2P)2 · · · · O*W*(3)^{viii}	2·769
O(2′)1 · · · · O*W*(7)^{iv}	2·622	O(2P)2 · · · · O*W*(3)^{v}	2·868
O(3′)1 · · · · O*W*(5)1^{iv}	3·084	O(1P)2 · · · · O*W*(1)^{v}	2·717
O(5′)1 · · · · N(1)3^{v}	3·086	N(1)3 · · · · · O*W*(2)^{v}	2·666
O(5′)1 · · · · O*W*(6)^{vi}	2·951	O*W*(1) · · · · O*W*(7)	2·751
O(5′)1 · · · · O*W*(5)	2·987	O*W*(2) · · · · O*W*(7)	3·054
O(1P)1 · · · N(6)3^{v}	2·894	O*W*(4) · · · · N(6)1	2·731
O(1P)1 · · · O*W*(2)	2·708	O*W*(6) · · · · O*W*(5)1^{iv}	2·627
O(2P)1 · · · O(3′)3	2·678	O*W*(6) · · · · O*W*(5)2^{iv}	2·685
O(2P)1 · · · O*W*(1)	2·872	O*W*(3) · · · · O*W*(3)^{v}	3·046
O(2P)1 · · · O*W*(6)	2·790	O*W*(3) · · · · O*W*(5)1	2·553
N(1)2 · · · · O(2′)3^{ii}	2·851	O*W*(3) · · · · O*W*(5)2	2·597
N(6)2 · · · · O(1P)2^{v}	2·976	O*W*(5)1 · · · O*W*(7)	2·931
N(6) · · · · · N(7)3^{v}	3·039		

Symmetry code

Super-script				Super-script			
None	x,	y,	z	(v)	y,	x,	$-z$
(i)	$1\frac{1}{2}-x$,	$-\frac{1}{2}+y$,	$\frac{1}{4}-z$	(vi)	$\frac{1}{2}-x$,	$-\frac{1}{2}+y$,	$\frac{1}{4}-z$
(ii)	$1+x$,	y,	z	(vii)	y,	$1+x$,	$-z$
(iii)	$1\frac{1}{2}-x$,	$\frac{1}{2}+y$,	$\frac{1}{4}-z$	(viii)	x,	$1+y$,	z
(iv)	$\frac{1}{2}-x$,	$\frac{1}{2}+y$,	$\frac{1}{4}-z$				

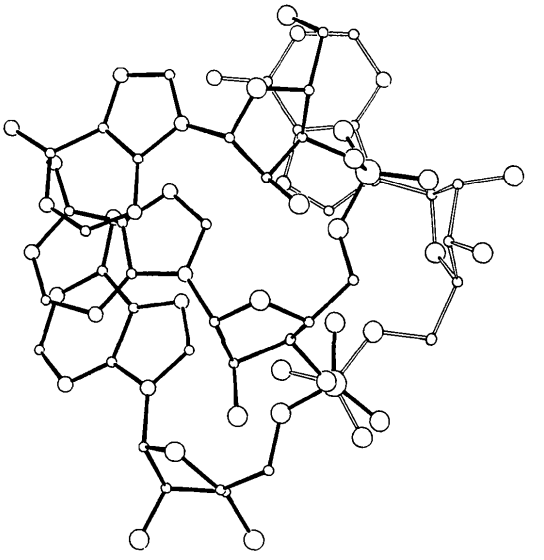

Fig. 6. Projection of the $ApA^{+}pA^{+}$ molecule along **c**. The 3′-terminal adenosine is drawn at its actual position (open bonds) and at a position corresponding to a helical conformation of the 3′-end (filled bonds). Atom designation as in Fig. 5.

base pairing in ApApA, a schematic comparison between ApApA and poly A, and a stereo view of the ApApA dimer with the surrounding water molecules. Fig. 10 is a stereo view of the packing of the ApApA dimers in the cell, Fig. 11(*a*) shows the poly A single helix constructed from the helical part of the ApApA molecule, and Fig. 11(*b*) a view along the helix axis.

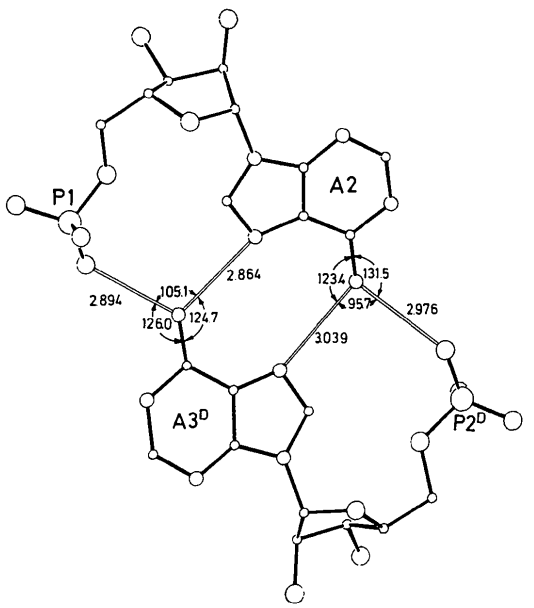

Fig. 7. Geometry of the base pair in the ApA^+pA^+ dimer. Hydrogen bonds indicated by open lines. Atom designation as in Fig. 5.

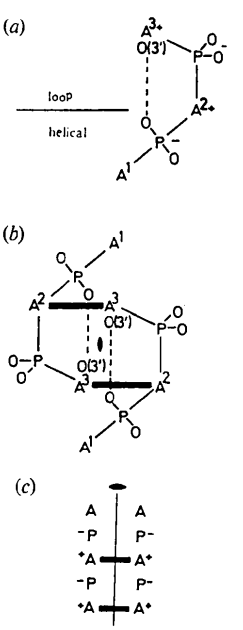

Fig. 8. Schematic drawings of structural features of the ApA^+pA^+ molecule: (*a*) folding back of the monomer; (*b*) the structure of the duplex; (*c*) the expected poly(A^+).poly(A^+)-like duplex structure.

We have adopted the usual numbering scheme for the adenine and ribose moieties (see Fig. 4). For brevity, the 5′-terminal, middle and 3′-terminal adenosines will be referred to as A1, A2 and A3, respectively. $A1^D$, $A2^D$ and $A3^D$ designate the corresponding nucleosides related by the symmetry operation $y,x,\bar{z}$, that is, the diad perpendicular to **c**.

Geometry of the ApApA molecule

(*a*) *Adenine rings.* With a few exceptions, bond angles and distances within the adenine bases are close to averaged values for protonated and unprotonated adenine heterocycles, respectively (Voet & Rich, 1970) (Fig. 4). The slight distortion in bonds and angles around C(5) and C(6) of A1 may be partly due to the higher thermal motion of the 5′-terminal adenosine. As will be discussed below, only a proton at N(1) of A3 could be located unambiguously from a difference map. It is not possible to decide on the basis of the observed bond angles and distances whether A2 is protonated or not.

Inspection of Table 3 shows that the bases are not exactly planar, the largest deviations being in A3, especially of C(6)3 (0·05) and N(6)3 (0·138 Å).

(*b*) *Riboses.* Within the three riboses the angles and distances are consistent and their averaged values are in good agreement with averaged values for other C(3′)-*endo* ribose units (Saenger & Eckstein, 1970). The C(5′)–O(5′) distance in A1 (1·385 Å) is significantly shorter than the corresponding bonds in A2 and A3, which may be attributed to the fact that there is no phosphate group attached to O(5′)1.

(*c*) *Phosphodiester groups.* The geometry of the two phosphodiester groups is characteristic for the negatively charged species and compares well with data published for dinucleoside phosphates. The distances to the unesterified O atoms are around 1·48, whereas the P–O ester bonds are near 1·60 Å (Fig. 4). The O(1P)–P–O(2P) angles are about 104°, but the angle between the esterified O atoms is near 120°. For the UpA structure (Rubin *et al.*, 1972) it has been argued that the observed difference in P–O(3′) and P–O(5′) (0·03 Å) in one of the molecules is mainly a consequence of different conformations around these bonds. We find differences of the same magnitude in these bonds, although the conformations are the same.

Charge distribution in ApApA

ApApA has been crystallized at *p*H 3 and one therefore should expect the phosphate groups to be negatively charged and at the same time the adenine heterocycles to be protonated at the N(1) atoms. Indeed, the geometry of the phosphodiester groups clearly suggests that they bear negative charges (see above). Since there are no counterions present in the crystal structure, only two of the three adenine bases can be protonated to achieve neutrality. From a difference elec-

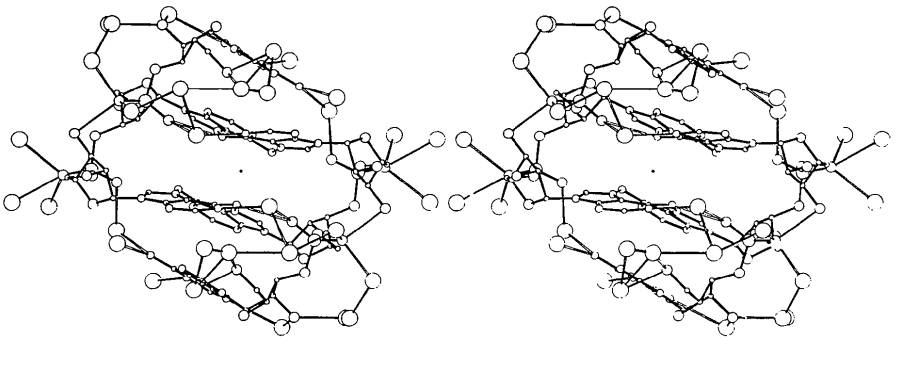

(*a*)

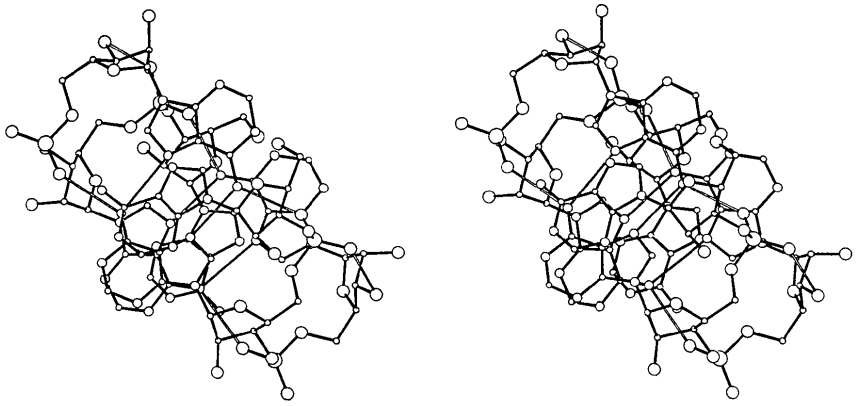

(*b*)

Fig. 9. (*a*) Stereo view of the dimer along the twofold axis. Atom designation as in Fig. 5. Largest circles represent H_2O molecules. (*b*) Stereo view of the dimer as seen along the *c* axis.

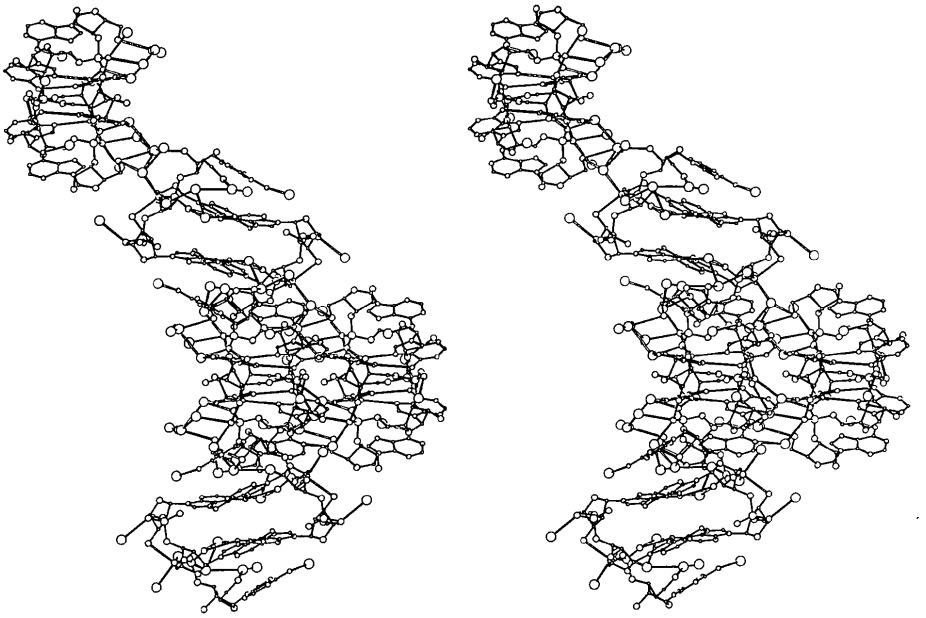

Fig. 10. Stereo projection of the crystal structure viewed along the diad. Open bonds represent hydrogen-bonding contacts, atom designation as in Fig. 5, largest circles represent H_2O molecules.

tron density distribution a proton at N(1)3 could be identified unambiguously. The fact that A2 and A3 are involved in the same interbase hydrogen bonding as described below, indicates that the 5′-terminal adenosine is *not* protonated. Thus the charge pattern of ApApA is that of an electrically neutral zwitterion with negatively charged phosphate groups and protonated middle and 3′-terminal adenine moieties:

$$(5'\text{-end})\quad A1p^{-}A2^{+}p^{-}A3^{+}\quad (3'\text{-end})\,.$$

Conformation of $ApA^{+}pA^{+}$; *helical and looped structures*

The conformational parameters of all three adenosine residues are essentially the same as those observed for double helical RNA's (Arnott, 1970) and nucleotides (Sundaralingam, 1973; Saenger, 1973). The orientation of the bases relative to the sugar is *anti*, as is clear from the torsion angles around the glycosidic bonds (Table 4). This torsion angle is identical within experimental error for A2 and A3, but is almost 20° smaller for the 5′-terminal residue A1. The same feature has been observed in the free acid form of UpA^{+} (Rubin *et al.*, 1972; Sussman *et al.*, 1972), in the sodium salts of ApU (Rosenberg *et al.*, 1973) and GpC (Day *et al.*, 1973) and the Ca^{2+} salt of GpC (Stellman *et al.*, 1975) and appears to be mainly an effect of the 5′-terminal position.

The conformation of the three ribose units is C(3′)-*endo* with C(3′) displaced by about 0·6Å from the least-squares planes through C(1′), C(2′), C(4′) and O(1′) (Table 3). The endocyclic dihedral angles (Table 4) differ only very little, demonstrating that the sugar puckering is almost identical for the three nucleosides.

The orientation of the C(5′)–O(5′) bonds is *gauche*, *gauche* (Table 4) as observed for all double helical nucleic acids (Arnott, 1970) and for all 5′-nucleotides (Sundaralingam, 1973; Saenger, 1973) except 6-aza-uridine-5′-phosphate (Saenger & Suck, 1973) and guanosine-5′-phosphate (Viswamitra & Seshadri, 1974). The most striking feature of the $ApA^{+}pA^{+}$ structure is the conformation of the phosphodiester bonds, which is different for the two phosphate groups. While the torsion angles around P1–O(5′)2 and P1–O(3′)1 are in the (−)*gauche* range, the corresponding angles in the second phosphodiester linkage are in the (+)*gauche* range. The angles for P1 are similar to those found for double helical RNA resulting in a helical $A1p^{-}A2^{+}$ fragment. The dihedral angles for the second phosphodiester group, on the other hand, are close to the values found for one of the UpA^{+} molecules and indicative of a non-helical structure. A consequence of this peculiar conformation of the $A2^{+}p^{-}A3^{+}$ fragment is a folding back of the 3′-terminal adenosine residue, which introduces a loop structure into the $ApA^{+}pA^{+}$ molecule and is stabilized through an intramolecular hydrogen bond between the O(3′) hydroxyl group of R3 and one of the unesterified O atoms at P1. The loop structure is clearly visible in Fig. 5. One should note the different orientations of the ribose residues which are indicated by arrows in the figure. Fig. 6 gives a view of the molecule in the

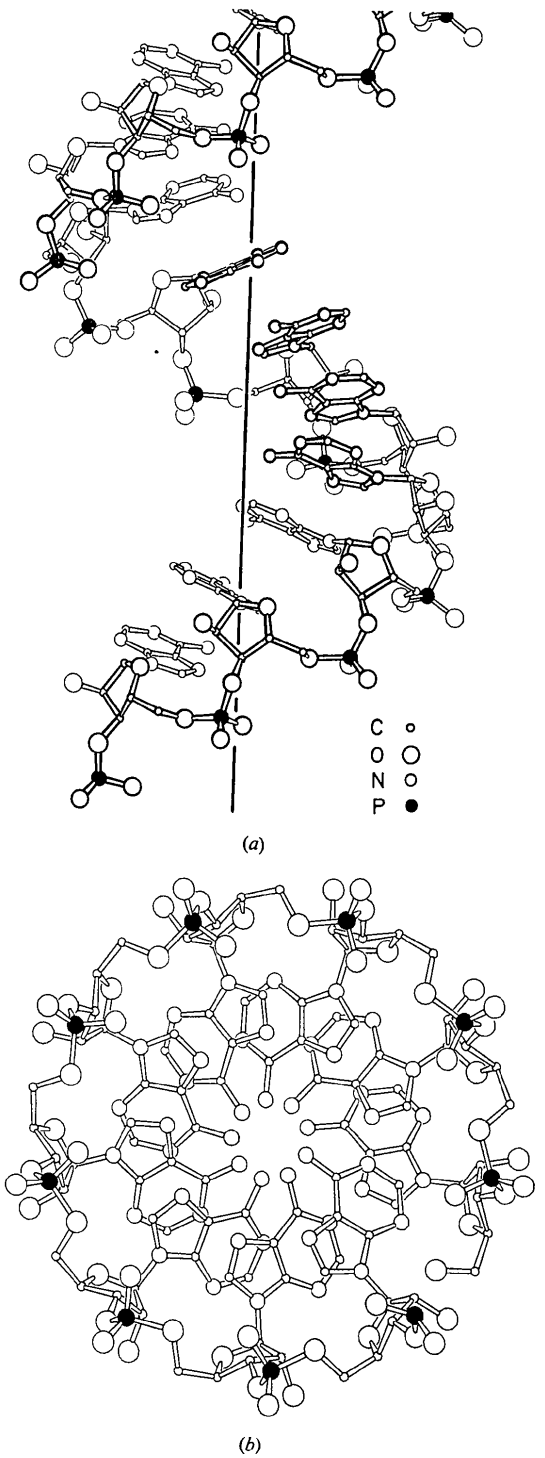

Fig. 11. The poly A single helix as derived from the $A1pA2^{+}$ fragment. (*a*) View perpendicular to helix axis, (*b*) along helix axis.

direction of the fourfold screw axis. The 3′-terminal adenosine is drawn in two positions corresponding to the actual conformation of P2 in the ApA^+pA^+ crystal structure and a hypothetical helical orientation of the 3′-end with the same P–O(ester) torsion angles as for the P1 phosphate group. It might well be that this peculiar loop structure with a hydrogen bond from the 3′-terminal 3′-OH group to the penultimate phosphate group also occurs in other oligonucleotides or polynucleotides and facilitates the recognition of 3′-termini in biological systems.

The ApA^+pA^+ *dimer*

As mentioned at the outset, we expected ApApA to crystallize from acidic solution as a poly A^+-like double helical fragment, shown schematically in Fig. 8(*c*). To form a double helical structure with the oligonucleotide chains *parallel* to each other, a twofold axis parallel to the helix axis and perpendicular to the base planes is required (Fig. 1). In the ApA^+pA^+ dimer, however, the diad is perpendicular to the stack axis and parallel to the base planes causing an antiparallel, non-double-helical orientation of the two oligonucleotide strands [Fig. 8(*b*)].

The two molecules of the ApA^+pA^+ dimer are related by a crystallographic twofold axis in the $P4_12_12$ crystals, but by a non-crystallographic pseudo-diad in the $P4_1$ crystals. The latter indicates that dimer formation already takes place in solution and is not a consequence of crystal packing forces. The two ApA^+pA^+ molecules of the dimer are linked by hydrogen bonds between the amino groups and the N(7) atoms of the protonated A2 and A3 adenine bases. In addition, there is a hydrogen bond between the amino groups and one of the free O atoms of the symmetry related phosphate group (Fig. 7). The ApA^+pA^+ dimer is stabilized by two of these base pairs. The same base-pairing scheme has been postulated for protonated double helical poly A^+.poly A^+ and has been found in the adenine layers of the UpA^+ crystals. In the poly A^+.poly A^+ duplex the base-paired adenines are related by a diad perpendicular to the base planes and coinciding with the helix axis but in the ApA^+pA^+ dimer, such a symmetry does not exist.

Stereoviews of the ApA^+pA^+ dimer along the diad and along the fourfold screw axis are shown in Fig. 9. The adenine base planes in ApA^+pA^+ are not exactly parallel to each other (see Table 3) and the base-paired adenine residues are tilted in a propeller-like fashion relative to each other forming an interplanar angle of 31·4°. This value is considerably larger than the 10° observed in UpA^+ and the 20° in double helical poly A^+.poly A^+.

While in the single ApA^+pA^+ molecule there is only minor base overlap between the 5′-terminal and middle adenine rings A1 and A2 (Fig. 5), there is extensive base overlap of the middle adenine rings of symmetry related molecules in the ApA^+pA^+ dimer. The A2 and $A2^D$ adenines are sandwiched between the 5′-terminal adenine rings, so that there is a continuous base stack formed along *c*. A3 and $A3^D$ show only vertical interactions of their C(6)–N(6) bonds (Figs. 9 and 10).

Hydrogen bonding and packing

Besides the hydrogen bonds forming the base-paired dimer, there are many short intermolecular contacts within the crystal structure involving almost all potential hydrogen-bond donor and acceptor atoms and especially the hydration water molecules. These contacts are listed in Table 5 with the symmetry operations involved. In contrast to A2 and A3, the 5′-terminal adenines A1 show no interbase hydrogen bonds, but they are in hydrogen-bonding contact with water molecules.

From the measured density it follows that there are six water molecules per ApA^+pA^+ molecule in the asymmetric unit. Difference maps revealed that one of the water molecules is statistically disordered, $OW(5)1$ and $OW(5)2$, at a distance of 1·55 Å from each other and occupancy factors of 0·36 and 0·32 respectively. The crystal water positions $OW(1)$, $OW(2)$, $OW(4)$ and $OW(6)$ are fully occupied, whereas the refinement of the occupancy factors for $OW(3)$ and $OW(7)$ converged at 0·70 and 0·65, respectively. Thus, the asymmetric unit contains the equivalent of six water molecules.

A stereo view of the ApA^+pA^+ dimer with the surrounding water molecules is shown in Fig. 9. These heavily hydrated dimers are the building blocks of the crystal structure and are aligned along **c** through the operation of the fourfold screw axis and interconnected through a net of hydrogen bonds. Fig. 10, a stereo view of the crystal structure, shows that base stacking along **c** is a dominant feature of this structure.

Conclusions

ApA^+pA^+ is the first trinucleoside diphosphate investigated by high resolution X-ray diffraction techniques. Several conclusions may be drawn from this analysis:

(1) The sugar phosphate backbone possesses considerable flexibility and may change its conformation abruptly from one phosphodiester linkage to the other.

(2) The occurrence of the same heavily hydrated dimer in $P4_12_12$ and $P4_1$ suggests that the duplex is present also in solution and that ApA^+pA^+ therefore adopts the non-helical conformation even at acidic *p*H. Formation of a double helical poly A^+-like fragment requires a critical nucleation length which is clearly beyond the trinucleoside diphosphate level.

(3) The intermolecular forces stabilizing the dimer in the crystal and in solution are interbase hydrogen bonding and vertical base stacking.

(4) The loop structure involving the 3′-terminal adenosine might be a general feature of polynucleotide 3′-termini and assist in the recognition of this part of the polymers by other biological systems.

(5) As mentioned in the introductory part, the sec-

ondary structure of poly A at neutral *p*H is not completely random but exhibits some single helical order for regions about 30–50 nucleotides long (Felsenfeld & Miles, 1967; Leng & Felsenfeld, 1966; Warshaw, Bush & Tinoco, 1965; Poland, Vournakis & Scheraga, 1966; Brahms *et al.*, 1966; Holcomb & Tinoco, 1965; Fresco, 1959). The $A1p^{-}A2^{+}p^{-}$ helical fragment of the $ApA^{+}pA^{+}$ molecule in this crystal structure can be considered as a representative part of a poly A single helix. Therefore, its two nucleotides were averaged by least-squares methods and from this 'idealized' fragment, a model for the structure of the poly A single helix could be derived (Saenger, Riecke & Suck, 1975). The helix is ninefold with a pitch height of 25·4 Å and the bases are tilted by 24° *versus* the helix axis, Fig. 11. The P atoms are at a radius of 8·07 Å, which renders the poly A single helix wider than the poly A^{+}.poly A^{+} double helix (radius = 5·95) but smaller than the A-RNA double helix (radius = 8·89 Å). As this model is the first developed for single-stranded nucleic acids, no comparison with existing models is possible.

The authors gratefully acknowledge the suggestion to study these crystals by Dr G. Weimann (Boehringer, Tutzing), help in the structure solution by Dr C. H. Schwalbe, Dr G. Germain and generous support and encouragement by Professor F. Cramer. D.S. and P.C.M. were recipients of fellowships from the Deutsche Forschungsgemeinschaft and Alexander von Humboldt Stiftung respectively. The computations were carried out at the Gesellschaft für wissenschaftliche Datenverarbeitung, Göttingen.

References

ARNOTT, S. (1970). *Progr. Biophys. Mol. Biol.* **21**, 265–319.
ARNOTT, S. & HUKINS, D. W. L. (1972). *Biochem. Biophys. Res. Commun.* **48**, 1392–1399.
BRAHMS, J., MICHELSON, A. M. & VAN HOLDE, K. E. (1966). *J. Mol. Biol.* **15**, 467–488.
BUSING, W. T., MARTIN, K. O. & LEVY, H. A. (1962). *ORFLS*. Oak Ridge National Laboratory Report ORNL-TM-305.
CAMERMAN, N., FAWCETT, J. K. & CAMERMAN, A. (1973). *Science*, **182**, 1142–1143.
DAY, R. O., SEEMAN, N. C., ROSENBERG, J. M. & RICH, A. (1973). *Proc. Natl. Acad. Sci. U.S.* **70**, 849–853.
FELSENFELD, G. & MILES, H. T. (1967). *Ann. Rev. Biochem.* **36**, 407–448.
FRESCO, J. R. (1959). *J. Mol. Biol.* **1**, 106–110.
GERMAIN, G. & WOOLFSON, M. M. (1968). *Acta Cryst.* B**24**, 91–96.
HOLCOMB, D. N. & TINOCO, I. (1965). *Biopolymers*, **3**, 121–133.
KARLE, J. & HAUPTMAN, H. (1956). *Acta Cryst.* **9**, 635–651.
LENG, M. & FELSENFELD, G. (1966). *J. Mol. Biol.* **15**, 455–466.
MAIN, P, GERMAIN, G. & WOOLFSON, M. M. (1971). *MULTAN, a System of Computer Programs for the Automatic Solution of Noncentrosymmetric Crystal Structures*, York, Louvain.
NORDMAN, C. E. (1966). *Trans. Amer. Cryst. Assoc.* **2**, 29.
POLAND, D., VOURNAKIS, J. N. & SCHERAGA, H. A. (1966). *Biopolymers*, **4**, 223–235.
RICH, A., DAVIES, D. R., CRICK, F. H. C. & WATSON, J. D. (1961). *J. Mol. Biol.* **3**, 71–86.
ROSENBERG, J. M., SEEMAN, N. C., KIM, J. J. P., SUDDATH, F. L., NICHOLAS, H. B. & RICH, A. (1973). *Nature, Lond.* **243**, 150–154.
RUBIN, J., BRENNAN, T. & SUNDARALINGAM, M. (1972). *Biochemistry*, **11**, 3112–3128.
SAENGER, W. (1973). *Angew. Chem. Int. Ed.* **12**, 591–601.
SAENGER, W. & ECKSTEIN, F. (1970). *J. Amer. Chem. Soc.* **92**, 4712–4718.
SAENGER, W., RIECKE, J. & SUCK, D. (1975). *J. Mol. Biol.* **93**, 529–534.
SAENGER, W. & SUCK, D. (1973). *Nature, Lond.* **242**, 610–611.
SEEMAN, N. C., DAY, R. O. & RICH, A. (1975). *Nature, Lond.* **253**, 324–326.
SHEFTER, E., BARLOW, M., SPARKS, R. A. & TRUEBLOOD, K. N. (1969). *Acta Cryst.* B**25**, 895–903.
STELLMAN, S. D., HINGERTY, B., BROYDE, S. B., SUBRAMANIAN, E., SATO, T. & LANGRIDGE, R. (1973). *Biopolymers*, **12**, 2731–2736.
STOUT, G. H. & JENSEN, L. H. (1968). *X-ray Structure Determination*, p. 457. London: Macmillan.
SUCK, D., MANOR, P. C., GERMAIN, G., SCHWALBE, C. H., WEIMANN, G. & SAENGER, W. (1973). *Nature New Biol.* **246**, 161–165.
SUNDARALINGAM, M. (1973). *The Jerusalem Symposium on Quantum Chemistry and Biochemistry*, Vol. **5**, pp. 417–456. Jerusalem: The Israel Academy of Sciences and Humanities.
SUSSMAN, J. L., SEEMAN, N. C., KIM, S. H. & BERMAN, H. M. (1972). *J. Mol. Biol.* **66**, 403–421.
TSAI, C., JAIN, S. C. & SOBELL, H. M. (1975). *Proc. Natl. Acad. Sci. U.S.* **72**, 628–632.
VISWAMITRA, M. A. & SESHADRI, T. P. (1974). *Nature, Lond.* **252**, 176–177.
VOET, D. & RICH, A. (1970). *Progr. Nucleic Acid Res. Mol. Biol.* **10**, 183–265.
WARSHAW, M. M., BUSH, C. A. & TINOCO, I. (1965). *Biochem. Biophys. Res. Commun.* **18**, 633–638.
WATSON, J. D. & CRICK, F. H. C. (1953). *Nature, Lond.* **171**, 737–739.